Retinal Vessels Segmentation Based on Enhancing Multi-scale Line Detection

Nguyen Mong Hien(✉)

Tra Vinh University, Trà Vinh, Vietnam
*hientvu@tvu.edu.vn

Abstract. Medical images are helpful for doctors to detect some dangerous diseases such as diabetes, age-related macular degeneration, hypertension, and arteriosclerosis. Abnormalities in retinal blood vessels cause these severe diseases. Thus, analysis of retinal vascular features is an excellent way to detect these abnormalities that help doctors make suitable treatment plans in the early stage. One of the retinal analysis tasks is retinal blood vessel segmentation which plays an important role because it needs to be done before any measurement can be created. In this paper, we proposed an approach for segmentation in retinal vessels by enhancing multi-scale line detection. The proposed method includes two steps. Firstly, the input image quality is improved using the Semi Translation Invariant Contourlet Transform (STICT). Finally, the result of the first step is applied by enhancing the multi-scale line detection technique (EMLD) to detect retinal blood vessels. As a result, our method can work effectively to segment more vessels. The performance of the proposed method evaluates both quantitatively and qualitatively on publicly available DRIVE dataset with an accuracy average reaching to 0.956. The result of the proposed method is better than the other methods.

Keywords: Retinal Blood Vessels · Segmentation · Line Detection · Retinal Vascular Features · Translation Invariant Contourlet Transform

1 Introduction

Retinal fundus images present different objects in the human retina. We sometimes face dangerous diseases such as hypertension, Diabetic Maculopathy (DM) and Diabetic retinopathy (DR), both of which come from the abnormal changes in the structure of these objects, especially in the retinal blood vessels. Evidence of this is some changes in vessel calibre caused hypertension [1, 2]. DR can be detected by the onset of neovascularization, being the early blindness symptom [3]. Arteriovenous nicking [4, 5] can cause a stroke.

These diseases are difficult to recognize in the early stage because of a lack of signs. These problems are presented clearly in the final stages. At that time, the treatment becomes more expensive and ineffective. Thus, retinal vessel change detection is essential to prevent the first step. As a result, this treatment becomes effective and cheap. The performance of medical diagnosis depends on accurate vessel segmentation because the accurate result consists of important clues contributing to the success of the following diagnosis processing.

Some different areas in the medical image are divided by the popular segmentation techniques based on colour, texture and intensity [6, 7]. The resulting image is helpful in identifying the objects. Other proper techniques are also used for segmenting medical images. Here they are threshold [8–12], combined both domain and threshold [13–16], deep learning [17–21], filter [22–25], clustering [26], etc. but the techniques have some drawbacks. Evidence of this, the techniques cannot work well in a few particular situations. For example, the retinal vessel image appears as a central light reflex or two vessels located nearby, or the vessels are very tiny, etc. To improve the segmented image quality, the limitations need to be handled.

Recently, researchers proposed some retinal blood vessel segmentation methods. However, their results have consisted of some limitations. For example, Staal [27] showed disconnected vessels. Soares [28] presented the vessels merging and the vessel splitting. Nguyen [29] proposed a method to segment the retinal blood vessel based on improving the salient region combined with the Sobel operator. The segmented images are low accuracy in the case of the vessel pixels with different saliency levels. Nguyen [30] introduced an effective method to segment the retinal blood vessels. However, the method also consists of some disadvantages. Both large vessels and tiny ones cannot be detected at the same time. Because the method only used one window size to classify a pixel belonging to the background or vessel. The window size contributes to the success of the line basic detection technique. Besides, with the tiny window size, a large vessel will divide into two tiny vessels. But, the two close tiny vessels will merge as larger vessels if the window size is set too large. Mustafa [31] introduced a retinal blood vessel segmentation technique better than the Kirsch templates' segmentation method. But, this method is not suitable for detecting tiny vessels.

Based on some of the mentioned limitations, an effective retinal blood vessel segmentation method is proposed to handle these drawbacks. This proposed method consists of two steps: applying STICT to enhance the source image quality and using MLD with different window sizes for vessel segmentation. Our proposed method is better than the current methods. The following sections consist of the background in Sect. 2, the proposed method in Sect. 3, the experiment results in Sect. 4 and the conclusion in Sect. 5.

2 Background

2.1 Translation Invariant Contourlet Transform

The contourlet transform includes two stages. The first stage is a Laplacian pyramid (LP) [32]. The second is a directional filter bank (DFB) [33]. In the first stage, an image is separated into some radial subbands plus an approximation image. In the second stage, the DFB is used for every detail subband where the highest number of directions are used for the finest subband, and to obtain the anisotropic scale rule of width a length, the number of directions levels is reduced at each other radial detail subband. Thus, the contourlet transform is realized by applying two stages of subsampled FBs to translate the invariant contourlet transform (TICT). The translation invariant (TI) schemes were developed to serve for translation invariant Laplacian pyramid (TILP) and translation invariant directional filter bank (TIDFB).

2.2   Line Detector

With a line detector [30], the image is divided into various channels: green, red and blue. The green channel is chosen to serve the line detector process. Because in the green channel, the vessels are brighter than the background. A window size W x W was applied to each pixel to calculate the grey level average at every pixel. The value is calculated as I_{avg}^{W}. The angular resolution decides the number of lines that pass through the centre pixel. This value of each line is calculated by averaging the pixel value.

The winning line has the highest value, shown by I_{max}^{W}. The line response of each pixel is calculated as Eq. (1):

$$R_w = I_{max}^{w} - I_{avg}^{w} \tag{1}$$

If a pixel has a high line response, the pixel will be the vessel pixel. The vessel consists of the pixels of the winning line. However, the pixel is considered a background pixel if its line response is low. The window size influences the performance of the method. This size of the window is double the calibre of the vessel.

This line detector technique is helpful for the light reflection situation. The value of the middle pixel is lower than the others in a large vessel. It makes the classification performance not high due to the tiny difference in the intensity values. But, the method found the pixels that belong to the vessel. A few central reflex pixels belong to the winning line. As a result, these pixels do not make the average value be dropped deeply. Therefore, the pixels are classified as vessel pixels thanks to the high response value. Moreover, the other pixels are considered background pixels thanks to applying the long-length lines. Although, the line detector technique is useful for retinal blood vessel segmentation. However, the technique cannot solve a few drawbacks, such as merging close vessels or dividing a large vessel into two smaller vessels.

3   Efficient Retinal Vessels Segmentation Based on EMLD

This part proposes an efficient retinal blood vessel segmentation method by applying EMLD. The generalized block diagram of the method is presented in Fig. 1.

Our method consists of two steps: denoising and segmenting the image. Each step will be presented in its subsection.

3.1   Denoising Image

In the first step, the original retinal image is converted into a grey image which is enhanced using STICT. This work should improve the input retinal image quality because this source retinal image usually consists of noise. This step can describe below:

 (i) This TILP is applied to partition the input retinal image into subbands. Each level of the TILP consists of four high-pass subbands.
(ii) To decrease redundant creation by the redundant transform of the TILP. The critically sampled DFBs applied to the TILP in the same way it was used to TIDFBs to realize the TICT. The technique is semi translation invariant contourlet transform (STICT).
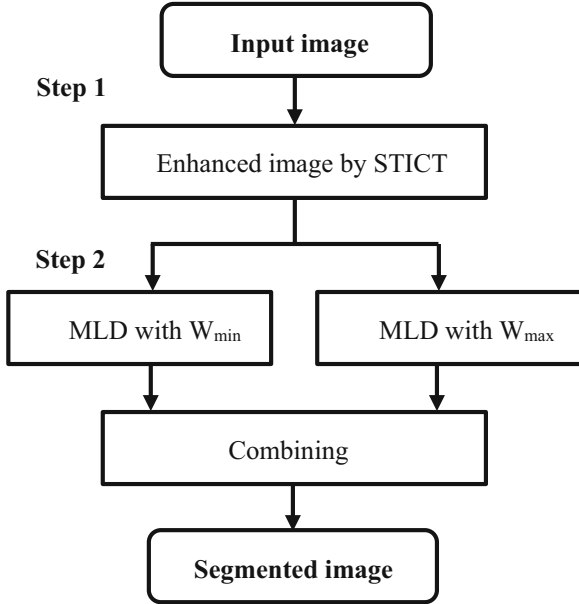
Fig. 1. The diagram of the method.

3.2 Segmenting Image

Recently, some researchers have proposed efficient medical image segmentation. Evidence of this, Nguyen [30] applied MLD to segment the vessels in the retinal image. According to the results, the technique is better than the primary line detection technique. However, this technique consists of some limitations. For example, the method cannot detect both large and small vessels. In particular, a few small vessels cannot be detected by the method because the method used only a window size during the detection process.

We, thus, proposed EMLD by applying the MLD with different window sizes. The basic line detector used to build the MLD. The line detector is computed by equation (2):

$$R_w^L = I_{max}^L - I_{avg}^w \tag{2}$$

where $1 \leq L \leq W, I_{max}^L$ and I_{avg}^W have the same meaning as the previous part. The values of L are controlled to implement the line detectors at various scales.

In our method, this maximum window size is applied to detect these large vessels, while the minimum window size is used to detect the small vessels. These window sizes are defined as W_{max} and W_{min} for the maximum window size and the minimum ones, respectively. Based on the vessel calibre, the window size will get a suitable value that approximates double vessel calibre.

It used Eq. (2) to detect both large and small vessels thanks to various suitable window sizes. Each window size has its benefits. With the W_{max}, the method can avoid dividing a large vessel into two small vessels. Moreover, the W_{min} applied to decrease some

limitations when a pixel of the background is located at a particular position. In fact, the background noise will increase if the line length is too short. The line responses at various scales are combined to avoid the situation. It is evident there is a slight difference among the raw response values that come from the line detector at each scale. Consequently, it is difficult to distinguish between the background and the vessels because of tiny differences. To differentiate between the background and the vessels easier, the raw response image values were standardized to make the unit standard deviation distribution and zero mean as Eq. (3):

$$R' = \frac{R - R_{mean}}{R_{std}} \tag{3}$$

R$'$ plays a role as the standardized response value, R plays a role as the value of the raw response, Rmean plays a role as the mean and R$_{std}$ as the standard deviation of the raw response value. This standardization has an important role in the distribution of intensity values. This technique is necessary for the response images produced by line detectors at different scales because its result is used for the combination process.

In the combination process, each scale has the same weight. The segmentation result is made by combining the line responses with various scales. The response at each pixel is defined by Eq. (4):

$$R_{combined} = \frac{1}{n_L + 1}\left(\sum_L R_w^L + I_{igc}\right) \tag{4}$$

where I_{igc} plays a role as the value of the inverted green channel at the corresponding pixel, n_L plays a role as the scale number, and $R_w{}^L$ plays a role as the line detector response at scale L. The green channel is integrated into the combination to distinguish the similarity between the blood vessels and other structures easier.

Lastly, the final segmented image combines the result images with different window sizes.

4   Experiment and Results

The DRIVE dataset [34] is used to evaluate the segmentation process. This dataset supplied some of the expert symptom assessment results that are considered standard to evaluate the results of the proposed method and the other methods.

The result of the segmentation process is made by classifying the pixel into a vessel or background. Therefore, in terms of the positive side, when a pixel is accurately classified into the vessel group, the event is considered as true positive (TP), and when a pixel is accurately classified into the background group, the event is considered true negative (TN). Regarding the negative side, when a pixel is incorrectly classified into the vessel group, the event is considered false positive (FP). When a pixel is incorrectly classified into the background group, the event is considered as false negative (FN).

The sensitivity and specificity are the statistical measures to evaluate the performance of methods [35]. The sensitivity is presented by Eq. (5), and the specificity is given by Eq. (6):

$$sensitivity = \frac{TP}{TP + FN} \tag{5}$$

$$specificity = \frac{TN}{TN + FP} \tag{6}$$

The accuracy is presented by Eq. (7):

$$accuracy = \frac{TP + TN}{P + N} \tag{7}$$

In the segmentation process, N is the sum of pixels that belong to the background, and P is the sum of pixels that belong to the vessel. The segmentation process's accuracy depends on the homogeneity level created by comparing the binary classification result and the ground truth. The segmentation method is considered effective when its accuracy is high.

In this study, the DRIVE dataset is used for the implementation; these ground truths vessels in the DRIVE dataset are used as a measurement standard to evaluate our method's and other methods' performance [30, 31]. Our proposed method runs twenty images in DRIVE. Two typical cases will be presented below.

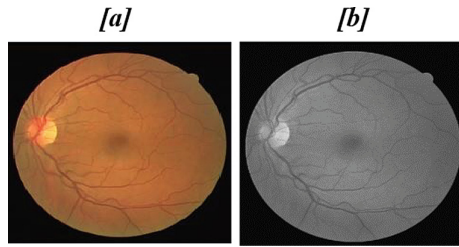These results are shown in Figs. 2, 3, 4 and 5. Each figure will be presented below:

[a]   [b]

Fig. 2. The input image and enhanced image.
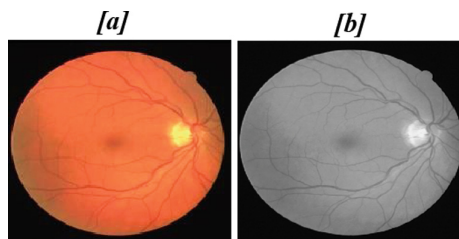
[a]   [b]

Fig. 3. The input image and enhanced image.

Figure 2a shows the input image, the result of the STICT technique shown in Fig. 2b. Moreover, Fig. 3a shows the input image, the result of the STICT technique shown in Fig. 3b. The technique should be done to enhance the quality of input image. It can make the input image reduce noise. This result is necessary for the next stage because the performance of EMLD will be low if the input image consists of noises. In other words, the line response of each pixel is calculated more accurately with the support of

the STICT. Based on the value, a pixel will be considered a vessel pixel or background pixel.

These results showed in Figs. 4 and 5. Figure 4a shows the input image, our result showed in Fig. 4b, the result of Nguyen [30] showed in Fig. 4c, and the result of Mustafa [31] is shown in Fig. 4d. Furthermore, the Fig. 5a shows the input image, our result showed in Fig. 5b, the result of Nguyen [30] showed in Fig. 5c and the result of Mustafa [31] showed in Fig. 5d.
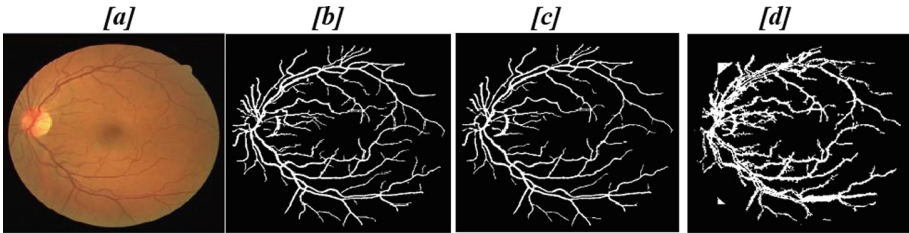
[a]   [b]   [c]   [d]

Fig. 4. The input image and segmented images.
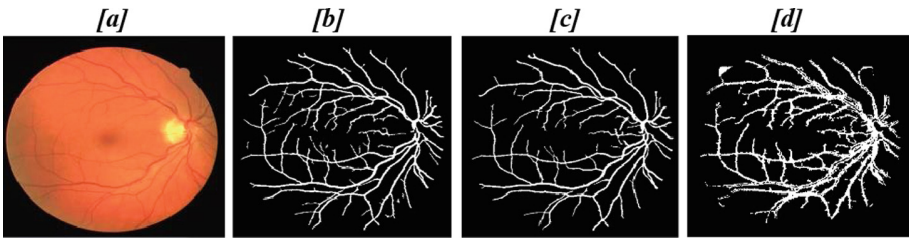
[a]   [b]   [c]   [d]

Fig. 5. The input image and segmented images.

According to the Figs. 4 and 5. It is clear that the segmented images of our method are better than the segmented images of other methods because our proposed method detected more vessels, thanks to applying STICT to enhance the quality of input image and use EMLD to segment vessels.

Table 1 presents the performance measures, including sensitivity, specificity, and accuracy. These parameter values are shown in italics when their values get highest.

Table 1. The first retinal blood vessel image.

Measures	Sensitivity	Specificity	Accuracy
Method [30]	67.89	98.92	95.48
Method [31]	68.45	94.89	91.78
Our method	*75.40*	*98.95*	*95.85*

Table 2. The second retinal blood vessel image.

Measures	Sensitivity	Specificity	Accuracy
Method [30]	71.88	98.41	96.07
Method [31]	65.67	95.94	92.86
Our method	*78.54*	*98.46*	*96.40*

To take insight from Tables 1 and 2, the performance of our proposed method is the best in all parameters, including sensitivity, specificity and accuracy. There is a big difference in sensitivity and a small difference in specificity and accuracy.

Table 3. The average results of our proposed method and other segmentation methods.

Measures	The average performance		
	Sensitivity	Specificity	Accuracy
Method [30]	62.91	98.78	94.89
Method [31]	61.09	95.39	91.27
Proposed method	*69.56*	*98.82*	*95.60*

All images in the DRIVE dataset serve to evaluate the average results that are made by applying our proposed method and recent segmentation methods. Based on the numbers in Table 3, we can easily recognize which method is the best in sensitivity, specificity, and accuracy. The average performance of our proposed method is the best in all measures.

5   Conclusions

With some dangerous diseases, the doctor needs to use segmented medical images that supply more clues related to medical problems. The paper proposes an efficient method to separate the blood vessels from retinal images. Our method includes two steps: apply the STICT to improve the quality of the source image and use MLD with different window sizes to detect vessels. This method can detect more vessels thanks to applying the two window sizes. This brings us to the conclusion that our retinal image segmentation method is more effective than recent ones according to computing these performance measures.

Conflict of Interest. The author declares that they have no conflict of interest.

References

1. Wasan, B., Cerutti. A., Ford, S., Marsh, R.: Vascular network changes in the retina with age and hypertension. J. Hyperten. **13**(12), 1724–1728 (1995)

2. Wong, T.T., McIntosh, R.: Hypertensive retinopathy signs as risk indicators of cardiovascular morbidity and mortality. British Med. Bull. **73**(1), 57–70 (2005)

3. Sussman, E.J., Tsiaras, W.G., Soper, K.A.: Diagnosis of diabetic eye disease. JAMA. J. Am. Med. Assoc. **247**(23), 3231–3234 (1982)

4. Wong, T.Y., et al.: Retinal microvascular abnormalities and incident stroke: the atherosclerosis risk in communities study. The Lancet **358**(9288), 1134–1140 (1982)

5. Wong, T.Y., et al: Retinal arteriolar diameter and risk for hypertension. Ann. Int. Med. **140**(4), 248–255 (2004)

6. Kaur, D., Kaur, Y.: Various image segmentation techniques: a review. Int. J. Comput. Sci. Mob. Comput. **3**(5), 809–814 (2014)

7. Ronneberger, O., Fischer, P., Brox, T.: U-Net: convolutional networks for biomedical image segmentation. In: International Conference on Medical Image Computing and Computer-Assisted Intervention, pp. 234–241 (2015)

8. Al-amri, S.S., Kalyankar, N.V., Khamitkar, S.D.: Image segmentation by using thereshod techniques. J. Comput. **2**, 83–86 (2010)

9. Marín, D., Aquino, A., Gegundez-Arias, M.E., Bravo, J.M.: A new supervised method for blood vessel segmentation in retinal images by using gray-level and moment invariants based features. IEEE Trans. Med. Imaging **30**(1), 146–158 (2011)

10. Evelin Sujji, G., Lakshmi, Y.V.S., Wiselin Jiji, G.: MRI brain image segmentation based on thresholding. Int. J. Adv. Comput. Res. **3**, 97–101 (2013)

11. Joshi, G.D., Sivaswamy, J., Krishnadas, S.R.: Optic disk and cup segmentation from monocular color retinal images for glaucoma assessment. IEEE Trans. Med. Imaging **30**(6), 1192–1205 (2011). https://doi.org/10.1109/TMI.2011.2106509

12. Li, X., Du, Z., Huang, Y., Tan, Z.: A deep translation (GAN) based change detection network for optical and SAR remote sensing images. ISPRS J. Photogramm. Remote. Sens. **179**, 14–34 (2021)

13. Hamdi, M.A.: Modified algorithm marker-controlled watershed transform for image segmentation based on curvelet threshold. Can. J. Image Process. Comput. Vis. **2**(8), 88–91 (2011)

14. Reddy, P.N., Mohan Rao, C.P.V.N.J., Satyanarayana, C.: Brain MR image segmentation by modified Active contours and Contourlet transform. ICTACT J. Image Video Process. **8**(2), 1645–1650 (2017)

15. Welikala, R.A., et al.: Automated arteriole and venule classi cation using Deep Learning for retinal images from the UK Biobank cohort. Comput. Biol. Med. **90**, 23–32 (2017)

16. Li, L., Verma, M., Nakashima, Y., Kawasaki, R., Nagahara, H.: Joint learning of vessel segmentation and artery/vein classification with post-processing. In: Proceedings of the International Conference on Medical Imaging with Deep Learning, vol. 121, pp. 1–14 (2020)

17. Holger, R.R., et al.: Deep learning and its application to medical image segmentation. Med. Imag. Technol. J. **36**(2), 1–6 (2018)

18. Qureshi, T.A., Habib, M., Hunter, A., Al-Diri, B.: A manually-labeled, artery/vein classified benchmark for the DRIVE dataset. In: Proceedings of the 26th IEEE International Symposium on Computer-Based Medical Systems, pp. 485–488 (2013). https://doi.org/10.1109/CBMS.2013.6627847

19. Binh, N.T., Hien, N.M., Tin, D.T.: Improving U-Net Architecture and Graph Cuts Optimization to Classify Arterioles and Venules in Retina Fundus Images. pp. 4015–4026 (2022)

20. Xu, X., Ding, W., Abra'moff, M.D., Cao, R.: An improved arteriovenous classification method for the early diagnostics of various diseases in retinal image, Computer Meth. Programs Biomed. **141**, 3–9 (2017)

21. Huang, F., Dashtbozorg, B., Tan, T., Romeny, B.M.H.: Retinal artery/vein classification using genetic-search feature selection. Comput. Methods Programs Biomed. **161**, 197–207 (2018). https://doi.org/10.1016/j.cmpb.2018.04.016

22. Li, Q., You, J., Zhang, D.: Vessel segmentation and width estimation in retinal images using multi-scale production of matched filter responses. Expert Syst. Appl. **39**(9), 7600–7610 (2012)

23. Permuter, H., Francos, J., Jermyn, I.: A study of Gaussian mixture models of color and texture features for image classification and segmentation. Pattern Recogn. **39**, 695–706 (2006)

24. Duchi, J., Hazan, E., Singer, Y.: Adaptive subgradient methods for on-line learning and stochastic optimization. J. Mach. Learn. Res. 2121–2159 (2011)

25. Liao, M., et al.: Efficient liver segmentation in CT images based on graph cuts and bottleneck detection. Phys. Med. **32**(11), 1383–1396 (2016)

26. Ng, H.P., Ong, S.H., Foong, K.W.C., Goh, P.S., Nowinski, W.L.: Medical image segmentation using k-means clustering and improved watershed algorithm. In: Proceedings of IEEE Southwest Symposium on Image Analysis and Interpretation, pp. 61–65 (2006)

27. Staal, J., Abràmoff, M.D., Niemeije, M., Viergever, M.A., Ginneken, B.V.: Ridge-based vessel segmentation in color images of the retina. IEEE Trans. Med. Imaging **23**(4), 501–509 (2004)

28. Soares, J.V.B., Leandro, J.J.G., Cesar, R.M, Jelinek, H.F., Cree, M.J.: Retinal vessel segmentation using the 2-d gabor wavelet and supervised classification. IEEE Trans. Med. Imaging **25**(9), 1214–1222 (2006)

29. Binh, N.T., Vo, T.H.T., Nguyen, M.H., Nguyen, T.T.: Retinal vessels segmentation by improving salient region combined with sobel operator condition. In: International Conference on Future Data and Security Engineering, pp. 608–617 (2019)

30. Nguyen, U.T.V., Bhuiyan, A., Park, L.A.F., Ramamohanarao, K.: An effective retinal blood vessel segmentation method using multi-scale line detection. Pattern Recogn. **46**, 703– 715 (2013)

31. Mustafa, W.A., Mahmud, A.S., Khairunizam, W., Razlan, Z.M., Shahriman, A.B., Zunaidi, I.: Blood vessel extraction using combination of kirsch's templates and Fuzzy C-Means (FCM) on retinal images. IOP Conf. Ser. Mater. Sci. Eng. **557**, 012009 (2019)

32. Burt, P., Adelson, E.H.: The laplacian pyramid as a compact image code. IEEE Trans. Commun. **com-31**(4), 532–540 (1983)

33. Bamberger, R.H., Smith, M.J.T.: A filter bank for the directional decomposition of images: theory and design. TEEE Trans. Sign. Process. **40**(4), 882–893 (1992)

34. Digital Retinal Images for Vessel Extraction. https://www.kaggle.com/datasets/andrewmvd/drive-digital-retinal-images-for-vessel-extraction/code. Accessed 5 April 2022

35. Vlachos, M., Dermatas, E.: Multi-scale retinal vessel segmentation using line tracking. Comput. Med. Imag. Graph. **34**, 213–227 (2010)